EFDA–JET–CP(09)06/62

K. McCormick, G. Maddison, C. Giroud, M. Beurskens, A. Boboc, S. Brezinsek, T. Eich, W. Fundamenski, S. Jachmich, M. Stamp, H. Thomsen and JET EFDA contributors

Coupling between JET Pedestal n_e –T_e and Outer Target Plate Recycling: Consequences for JET ITER-Like-Wall Operation

Coupling between JET Pedestal $n_e - T_e$ and Outer Target Plate Recycling: Consequences for JET ITER-Like-Wall Operation

K. McCormick[1], G. Maddison[2], C. Giroud[2], M. Beurskens[2], A. Boboc[2], S. Brezinsek[3], T. Eich[1], W. Fundamenski[2], S. Jachmich[4], M. Stamp[2], H. Thomsen[1]
and JET EFDA contributors*

JET-EFDA, Culham Science Centre, OX14 3DB, Abingdon, UK

[1]Max-Planck IPP, EURATOM Association, D-85748 Garching, Germany.
[2]EURATOM/UKAEA Fusion Association, Culham, Abingdon, Oxon. OX14 3DB, UK
[3]FZ Jülich GmbH, Institut für Plasmaphysik, Association EURATOM-FZJ, Jülich, Germany
[4]Association EURATOM-Belgian State, Koninklijke Militaire School - Ecole Royale Militaire, B-1000 Brussels Belgium
** See annex of F. Romanelli et al, "Overview of JET Results", (Proc. 22nd IAEA Fusion Energy Conference, Geneva, Switzerland (2008)).*

Preprint of Paper to be submitted for publication in Proceedings of the
36th EPS Conference on Plasma Physics, Sofia, Bulgaria.
(29th June 2009 - 3rd July 2009)

1. INTRODUCTION

With the tungsten target plates of the JET ITER-Like-Wall (ILW) phase, carbon radiation will be reduced and must be replaced by that of seeded impurities to prolong target plate lifetime. Investigations to this end of ELMy-H (EH) & Advanced Tokamak (AT) scenarios using N_2 and Ne along with D_2 fuelling have been carried out in matrix fashion Figure 1 top), whereby the aim was to cover a large variation in divertor power loading P^{div} and temperature T_e^{div} regardless of core performance. The intended effect of impurity seeding is to increase radiation P_{rad} in order to mitigate P_{div} and that of D_2 to enhance recycling to further reduce T_e^{div}, both being necessary for ILW-compatibility. P_{rad}/P_{in} ranged over 48-66% (EH) and 31-60% (AT). Details on P_{rad} and P_{div} are given in a companion paper [1]. This data set is used to study the interrelationships between the pedestal temperature T_e^{ped} & density n_e^{ped} and the ion flux G_i to the outer target plate. An advantage of these studies is the wider range of neped and T_e^{ped} afforded by the use of impurities. Different type-I ELM regimes also prevail: For EH, ν_{ELM} initially decreases with D_2 (~20->10Hz). Impurities can provoke compound ELMs ($\nu_{ELM} \geq 3$Hz) as well as augment ν_{ELM} (to 50Hz).

2. EXPERIMENTAL RESULTS

All quantities reported are averaged over ~1s, i.e. over many ELM cycles. This is readily done using T_e from the ECE radiometer, with the values deviating less than 50eV (<5%) from those gained from the High Resolution Thomson Scattering (HRTS) system. As radiometer values were not always available, T_e from HRTS is cited, read at the 90% flux surface. Inter-ELM Te-excursions in compound ELM phases can more than 200eV (only with N_e in EH) with an average deviation from the mean of <±100eV, otherwise ~±50eV. The edge vertical interferometer channel (tangent to 90% flux surface) also enables good time averaging, has a low noise level and none of the potential calibration uncertainties associated with Thomson scattering. It is very closely related to ne from HRTS and is taken to define neped, with a typical uncertainty of $\pm 10^{18}$ m^{-3}. A rough estimate of Γ_i is obtained from the D_α line intensity summed over the outer target plate $\Phi_{D\alpha}$ using S/XB~30, i.e. $\Gamma_i = 30\ \Phi_{D\alpha}$. An estimate of T_e^{div} is derived from P_{div}^{out} (IR camera) and Γ_i: $T_e^{div} = P_{div}^{out}$ $/(8\Gamma_i \times 1.6\times10^{-19})$, 8 = energy transmission factor. Langmuir probe results from other EH discharges indicate this quantity need be multiplied by 2 to obtain the peak T_e. Values for T_e^{div}, energy confinement time τ_E, T_e^{ped} and neped are plotted versus. Γ_i in fig. 3. Note, Γ_i is largely determined by D_2 (fig.1). Higher Γ_i means lower τ_E, with impurities often making matters worse (fig.3), in particular at lowest Γ_i where a dramatic drop in neped can occur (also in T_e^{ped} for AT Ne-seeding), associated with an impurity-driven increase in Ω_{ELM}. Seeded Ne or N_2 leads to an obvious enhancement of P_{rad} only at lower Γ_i (-> lower D_2) for the present carbon-dominated environment (50->61% for EH, 30->60% for AT) [1]. Evidently T_e^{ped} is not reduced by P_{rad} cooling as one might expect (fig.3); it does decrease uniformly with higher Γ_i, showing minor impurity variations. In contrast, n_e^{ped} initially increases with Γ_i (D_2 fuelling), then rolls over.

3. DISCUSSION:

SOLPS code calculations for a density scan at constant power (5MW, inner & outer strike points on horizontal target) may be used to examine how the values of $D\alpha$ code and ìi code are related [2]. The result is for T_e^{div}>4eV $D\alpha$~Γ_i 0.76, i.e. S/XB = Γ_i code/$D\alpha$ code is not constant (due in part to the S/XB Te dependence). Nonetheless, $D\alpha$ code still mirrors ìi code over a wide range of T_e^{div}, implying that the assumption S/XB = 30 is a credible approach to gain a first estimate of the experimental ìi from the measured $D\alpha$. Taking the separatrix density nes from HRTS, using a Tanh fit in the gradient region and assuming the separatrix position is correctly given by EFIT, yields the relationship $\Gamma_i \sim n_{es}^{2.5\pm0.3}$ for both EH & AT. This signifies that Γ_i is a very sensitive probe for changes in n_{es}, n_{es} being more difficult to measure with precision due to the steep gradients in the edge region and uncertainty in separatrix location.

Figure 4 illustrates that Γ_i (e.g. n_{es}) is closely correlated with n_e^{ped}/τ_E, meaning an enhancement in Γ_i dictates an increase in n_e^{ped} and/or a decrease in τ_E must prevail (τ_E is intertwined with the D2- & impurity-levels). Another correlation exists between Γ_i and n_e^{ped}/T_e^{ped} (fig.4). A least-squares regression (not accounting for errors in n_e^{ped} & T_e^{ped}) yields good fits (given in the fig.5 caption) to Γ_i over the entire operational ranges for both ELMy-H and AT scenarios.

These encompass an order of magnitude change in Γ_i and a factor of ~2 for n_e^{ped}/T_e^{ped}. The exact form of the fits is not of importance here, rather the demonstration of the very coherent interplay among τ_E-n_e^{ped}-T_e^{ped} and Γ_i, illustrated in figs. 4 and 5, i.e. a coupling over the Edge Transport Barrier (ETB) region between the core/pedestal and Γ_i to the outer target plate (and thus n_{es}). In addition, the estimated n_{es} values won from HRTS are found to be nearly linear with n_e^{ped}/τ_E for both EH & AT (not shown). These are new observations of fundamental nature, implying that any change in ìi is automatically accompanied by a change in τ_E-n_e^{ped}-T_e^{ped} along the operational curves defined by the points of figs. 4 & 5 and vice versa.

CONCLUSIONS

The discovered link among τ_E-n_e^{ped}-T_e^{ped} and Γ_i (e.g. n_{es}) suggests a phenomenon such as "stiff profiles" could be in action in the ETB, perhaps in combination with a critical gradient related to ELM onset conditions. This remains to be examined. Stiff ETB profiles have been observed on ASDEX-Upgrade, with η_e~2 being common [3]. In any case, the observed coupling, whatever its origin, has ramifications when producing ILWcompatible conditions at the target plate: Enhanced Γ_i will be obligatory to suppress T_e^{div} to tolerable levels (exact value to be determined at the start of ILW operation) and also to secure reasonable plasma operation in the presence of mandatory seeded impurities. Higher Γ_i is achievable only through D_2 fuelling - leading to higher n_{es} - and through the coupling to higher n_e^{ped}/τ_E or n_e^{ped}/T_e^{ped}. This chain of events appears unavoidable.

A corollary is that the increase in neutral pressure associated with higher D_2 does not necessarily lead to a lower τ_E because of penetration to the pedestal and reduction of T_e^{ped}. Rather, the change in pedestal parameters is a result of constraints imposed by the established interconnections in association with the change in n_{es}. Similarly, an alteration in pedestal confinement – due to modes, for example, present in some of the selected discharges [1] or due to the addition of impurities – will also effect a modification of n_{es} and Γ_i.

ACKNOWLEDGEMENTS

Work conducted under EFDA and partly supported by the UK Engineering & Physical Sciences Research Council and the European Community under the contract of Association between EURATOM and UKAEA. The views and opinions expressed herein do not necessarily reflect those of the European Commission.

REFERENCES

[1]. G. Maddison *et al.*, Paper P2.160 this conference

[2]. D. Coster, private communication

[3]. A. Kallenbach *et al.*, Nuclear Fusion **43** (2003) 573; J.Neuhauser *et al.*,Plasma Physics Controlled Fusion **44** (2002) 855

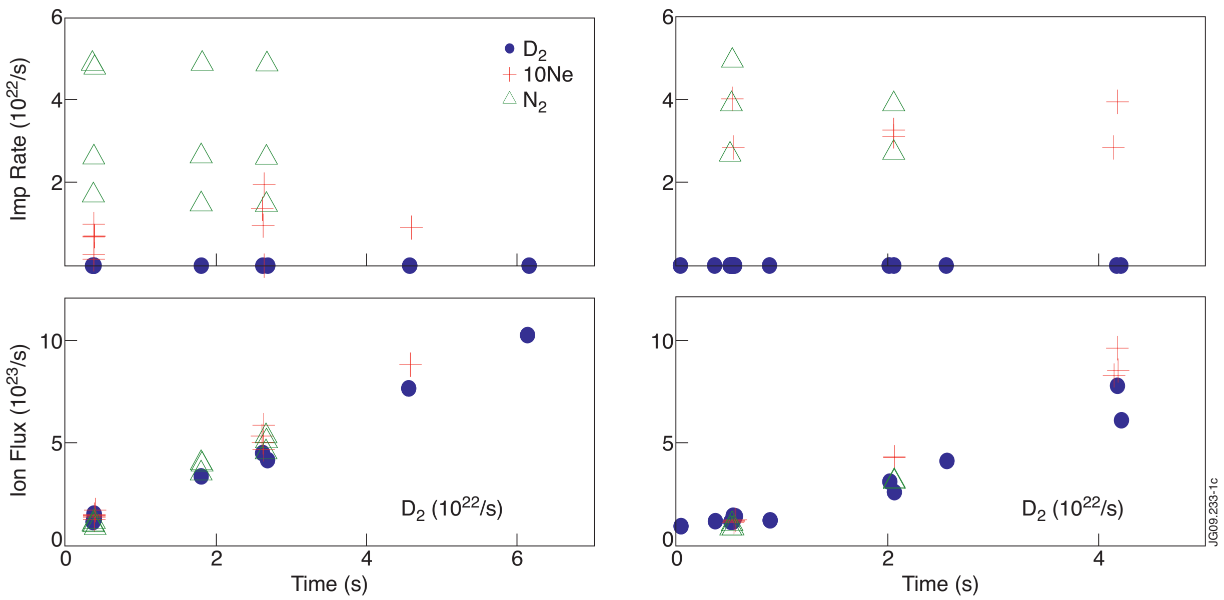

Figure 1:Impurity electron rate & ion flux to the outer target plate versus D_2 electron rate. Ne-rate multiplied by 10. Left: ELMy-H; Right AT.
EH: *~ 16MW, 2.5MA, 2.7T, q_{95} ~ 3.5, n_{eGW}~0.65-1.07, $H_{98y,2}$ ~ 0.8-1.09;*
AT: *~ 23MW, 1.75MA, 2.7T, q_{95} ~ 5, n_{eGW}~0.41-0.79, $H_{98y,2}$ ~ 0.66-1.02. NBI electron fuelling ~1.1 10^{21}/s (EH) & 1.8 10^{21}/s (AT).*

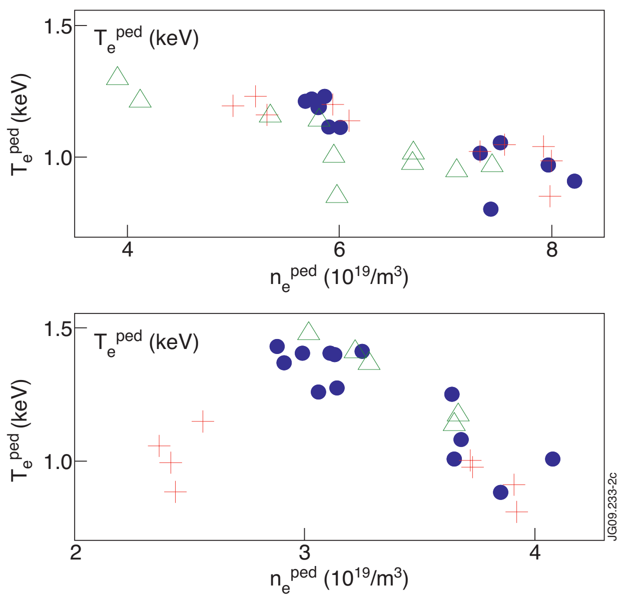

Figure 2: Pedestal T_e^{ped} versus n_e^{ped}. dot = D_2 fuelling, plus = D_2+Ne, triangle = D_2+N_2 Top ELMy-H; Bottom AT.

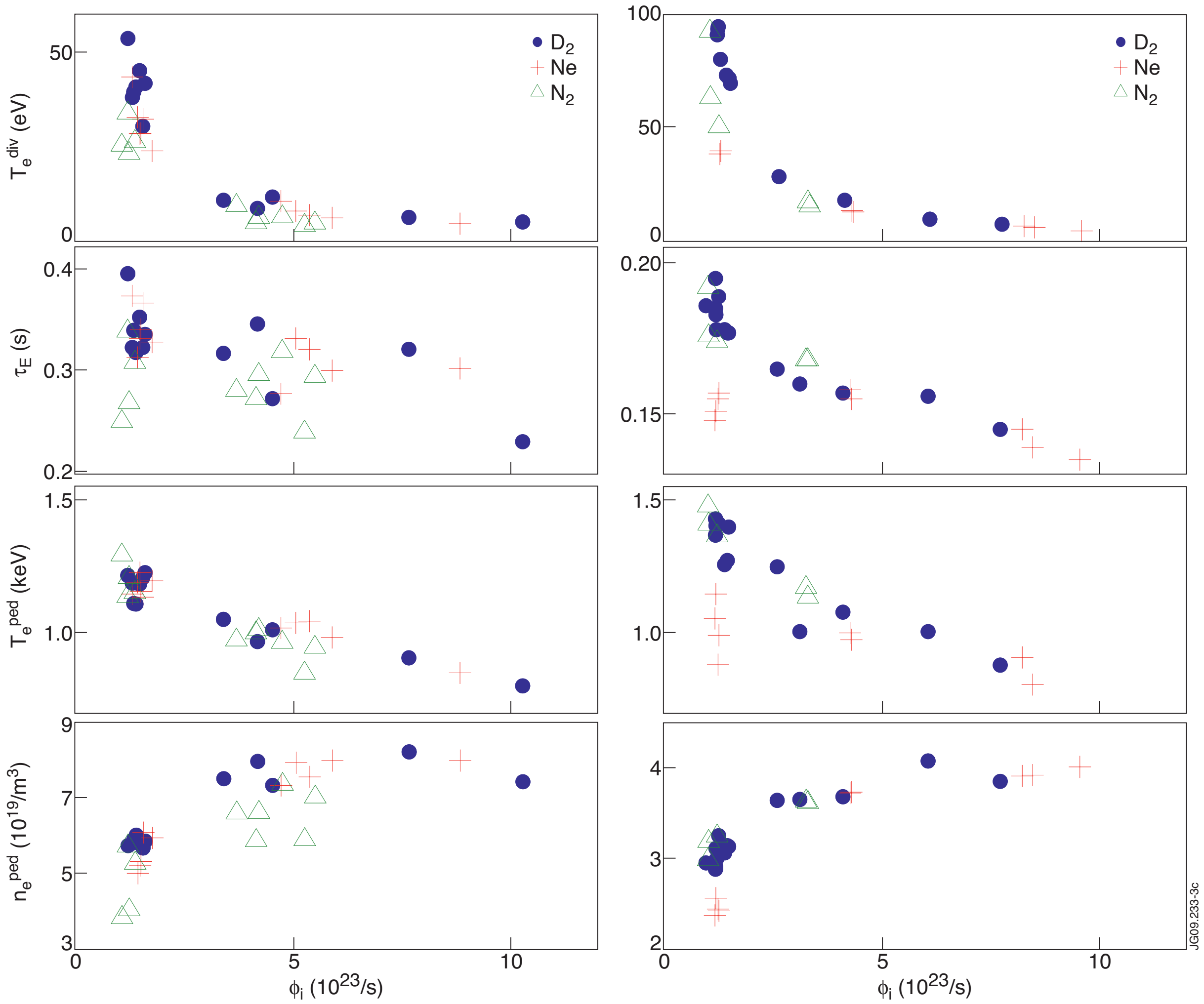

Figure 3: top to bottom, all versus ion flux to target plate Γ_i: T_e^{div} computed from P_{div}^{out} & Γ_i using $T_e^{div} = 2\ P_{div}^{out}/(8 \times e \times \Gamma_i)$; energy confinement time τ_E,; T_e^{ped} & n_e^{ped}. Left ELMy-H; Right AT.

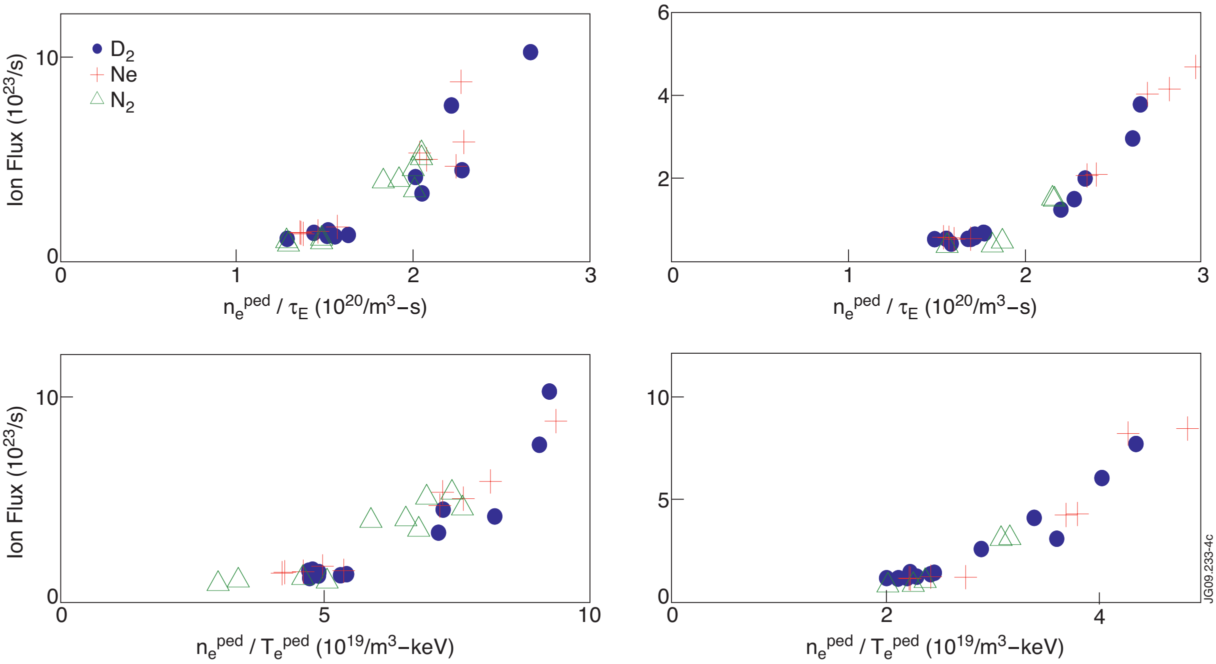

Figure 4: Ion Flux Γ_i to outer target plate versus n_e^{ped}/τ_E (top) & n_e^{ped}/T_e^{ped} (bottom). Left ELMy-H; Right AT.

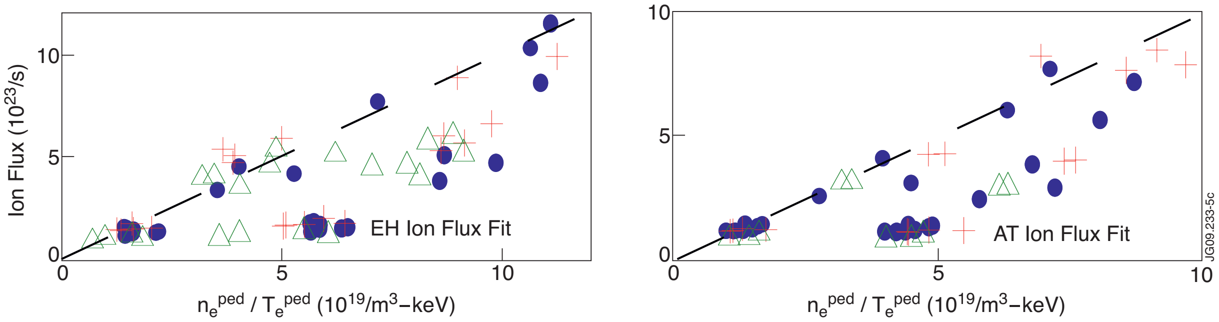

Figure 5: Γ_i versus fit: Left ELMy-H ($9.310^{13}\ n_e^{ped1.11\pm0.35}/T_e^{ped4.13\pm0.54}$);
Right AT($1.1710\text{-}30\ n_e^{ped3.08\pm0.21}/T_e^{ped\,2.22}\pm0.18$)[$m^{-3}$,eV]